Microchimica Acta (2019) 186:646
https://doi.org/10.1007/s00604-019-3745-6

ORIGINAL PAPER

A study on the electro-reductive cycle of amino-functionalized graphene quantum dots immobilized on graphene oxide for amperometric determination of oxalic acid

Praveen Mishra[1] · Badekai Ramachandra Bhat[1]

Received: 14 April 2019 / Accepted: 10 August 2019

Abstract
Amino-functionalized graphene quantum dots (NH_2-GQD) are described for the amperometric determination of oxalic acid. The NH_2-GQD were synthesized via a hydrothermal method using hexamethylenetetramine as the source for nitrogen. The average particle size of the GQD is ~30 nm, which is also supported by TEM. Electrochemical analysis of the NH_2-GQD-GO composite on a glassy carbon electrode at pH 7.4 showed a faint reduction peak at −0.6 V vs. SCE, which was enhanced in the presence of oxalic acid. This variation in cathodic current density is an interesting deviation from the usually studied anodic current density for the electrochemical sensors. This is also supported by cyclic voltammetry and time-based amperometric measurements. The electrode has a linear response in the 0.5–2.0 mM and 2.0–55 mM oxalate concentration ranges and a 50 μM detection limit (at $S/N = 3$). The electrode was successfully applied to the determination of oxalate in spiked urine samples.

Keywords Electrochemical analysis; cathodic current density · Cyclic voltammetry · Amperometery

Introduction

Graphene quantum dots (GQD), are virtually single or few atomic layers thick, fragmented graphene which possess strong quantum confinement and edge effects. This is reflected in their interesting wavelength-dependent photoluminescence (PL) phenomena. When compared to conventional quantum dots (QD) and carbon dots (CD), GQD are different with respect to the properties such as high surface area, larger diameter, better surface grafting using the π conjugated network or surface groups, and other physical properties arising due to its graphene structure [1]. Structure of GQD along with unique optical properties makes them excellent materials for the construction of nanoscale optical and electronic devices. GQD have been well studied for their synthesis methods as well as electronic and optical property tuning [2], and are also investigated for their application such as photovoltaic devices and electrochemical catalysis [3]. GQD have also been studied for their chemical and bio-sensing applications [4]. The sensing ability of GQD can be attributed to their photoluminescence or electrochemical property [5, 6]. They have been used to sense a wide range of analytes ranging like heavy metal ions [7–11], toxic anions [12–14], organic compounds [15], and biomolecules [16, 17]. Oxalic acid is commonly found molecules in various organisms like fungi, plants and animals. High concentration of oxalic acid is found to remove calcium from blood, which in turn have severe disturbances in the activity of heart and neural system. Normal range of oxalic acid in human body is 10–40 mg.24 h^{-1} in urine. However, in case of individuals with a metabolic disorder called hyperoxaluria, the amount of oxalic acid in their urine can be as high as 53–654 mg.24 h^{-1} [18]. This condition is often associated with kidney stone. Therefore, it is important to determine oxalic acid in bio fluids [19]. There are very few methods reported for the determination of oxalic acid or the oxalates in biological systems. Bergerman and Elliot

Electronic supplementary material The online version of this article (https://doi.org/10.1007/s00604-019-3745-6) contains supplementary material, which is available to authorized users.

✉ Badekai Ramachandra Bhat
brchandra@gmail.com; ram@nitk.edu.in

[1] Catalysis and Materials Laboratory, Department of Chemistry, National Institute of Technology Karnataka, Surathkal, Mangalore, Karnataka 575025, India

Published online: 26 August 2019

reported a reaction between oxalic acid and indole which led to photometric determination of oxalic acid [20]. Another related technique to determine oxalic acid in the biological system is fluorometric, colorimetric and spectrometric methods [21–23]. Chromatography is another suitable techniques which was explored for the determination of oxalic acid [24, 25]. Electrophoresis is another reported technique for determination of oxalic acid [26]. However, these methods require preparation of assays and thus are usually time consuming. A much more capable and fast sensors are thus needed in the modern age. Electrochemical sensors can meet this requirement. Few attempts have been made to fabricate such electrode among which bare platinum electrode and platinum nanoparticles decorated glassy carbon electrode have shown by far the best sensitivity for oxalic acid [27]. Bare platinum showed LOD of 0.38 μM whereas the modified glassy carbon electrode can detect oxalic acid as low as 0.28 μM. The graphene modified carbon ionic liquid electrode have shown to detect oxalic acid till 0.48 μM with a linear range of 8.00 μM to 6.00 mM [28]. Palladium nanoparticles loaded carbon nanofibers modified carbon paste electrode have shown a detection limit of 0.2 mM with linear ranges of 0.2–13 mM and 13–45 mM [29]. Similarly, platinum nanoparticles immobilized on polypyrrole nanofibers also presented as field-effect transistor type sensors for the determination of oxalic acid to femtomolar-level [30]. Irrespective of showing appreciable sensitivity towards the detection of oxalic acid, these electrodes are very expensive to fabricate given the use of rare earth metal or the stability and synthesis of ionic liquid. Another common precedence in electrochemical detection is the use of the variation in anodic current (oxidative cycle) for the determination of analyte. Here we report a two-step synthesis of amino functionalized GQD, which when forms suspension with graphene oxide (GO), is able to sense oxalic acid, which can be determined by electrochemical method. Graphene oxide is a 2-dimensional nanostructure which is loaded with oxygen rich functional group which makes its chemical modification possible [31]. The GO provides high surface area to adsorb the analyte, thus was selected as substrate for the composite. The presence of oxygen rich group in the system also enables us to utilize the cathodic current (reduction cycle) for analysis. This enables the electrode to be very responsive towards the presence of analyte. This method is developed to offer a potential alternative to the existing enzyme-based sensors.

Experimental

Synthesis of amino–functionalized GQD

Graphite was procured from Sigma Aldrich (https://www.sigmaaldrich.com/india.html). All the other reagents used in the experiment were purchased from Merck India (https://www.merckgroup.com/in-en). Graphene oxide (GO) was synthesized by the improved Hummer's method from natural flaked graphite [32]. The obtained graphene oxide and dispersed in 500 mL distilled water. GQD were prepared using the earlier reported Hydrothermal Cutting method [2]. The photoluminescence observed when the resulting product was irradiated with an electromagnetic wave of 365 indicated of the synthesis of GQD. Further GQD were functionalized using hexamethylenetetramine, where a dispersion of GQD in 0.1 M hexamethylenetetramine solution was refluxed at 80 °C for 4 h to yield amino functionalized GQD (NH_2-GQD). The NH_2-GQD-GO composite was synthesized by dispersing NH_2-GQD in GO suspension. GQD-GO composite was synthesized similarly by dispersing GQD in GO suspension.

Fabrication of the electrode

The NH_2-GQD-GO composite suspension was drop casted over the glassy carbon electrode (ø = 4.0 mm) followed by 4 h of drying in hot air oven at 60 °C to form the working electrode. This electrode was further used to study its suitability for the electrochemical determination of oxalic acid. For a comparison, GQD, NH_2-GQD and GO drop casted glassy carbon electrodes were also fabricated.

Material characterization

The X-ray diffraction pattern of Graphene oxide was characterized using Rigaku Mini Flex X-ray Diffractometer. Graphene oxide and GQD were examined under the Transmission electron microscopy (JEM-2100PlusTransmission Electron Microscope) for their morphology and size determination. The FTIR spectra of the samples were obtained using BRUKER FTIR spectrometer with Eco-ATR accessory. Raman spectra of the samples were obtained using a Renishaw Raman microscope using 514 nm laser excitation at room temperature.

Electrochemical analysis

All the electrochemical measurements were performed using Metrohm Autolab PGSTAT-30 electrochemical workstation using a three-electrode setup. Platinum wire was used as counter electrode and saturated calomel electrode (SCE) was reference electrode. The 0.2 M phosphate buffer (pH = 7.4) was used as electrolyte, which matches the pH of average urine sample. Scan rate for the all the measurement was 50 $mV.s^{-1}$. The voltage ranges for the cyclic voltammetry sweep from −1.0 V to 0 V with the start and end voltage of 0 V. For the electrochemical determination of the sample, 2 ml of sample (oxalic acid or urine) was added to the 20 ml of electrolyte. All the solutions were prepared using deionized water.

Choice of materials

GQD was selected as a sensing materials owing to its ease of synthesis. GQD are environmentally benign and do not pose any harmful effect to the humans. Structurally, the presence of amine group on the edge of functionalized GQD can act as site for binding di-basic carboxylic acid. These carboxylic acid groups present on the electrode surface then undergo electro-reduction. Oxalic acid was therefore selected as the model di-basic carboxylic acid due to its biological importance. The use of NH_2-GQD over other known materials such as known materials such as polypropylene, polyaniline, gold nanoparticles, and oxides and sulphides like ZnO and MoS_2, provides a direction to explore further use of GQD and functionalized as electrochemical sensors due to the ease of functionalization of its edges. Therefore, NH_2-GQD was selected to form NH_2-GQD-GO composite used for the electrochemical determination of oxalic acid.

Results and discussions

Characterization of GO and GQD

The GO synthesized by improved Hummer's method was analyzed for its X-ray diffraction pattern to confirm its successful synthesis. Presence of the characteristic broad peak at $2\theta = 11.5^o$ corresponding to the (001) plane of graphene oxide (Figure S1(A)) [32]. The peaks at $2\theta = 26.5^o$ and 54.5^o are of (002) and (004) planes of graphitic carbon sheets respectively (JCPDS Card No.75–1621). These peaks suggest that some of the layered graphite like structure have been retained in the GO. This is later illustrated in the TEM of NH_2-GQD (Fig. 1(a)). Additionally, the graphitic peak may also be due to trace nanographite which are retained with the graphene oxide. However, the small intensity of the graphitic peak suggests very low percentage of graphitic impurity in the GO. The transmission electron micrograph shows a typical sheet of GO (Figure S1(b)). GO sheets are often observed having varying layers [33]. Small ruptures in the GO sheets are due to the strong oxidation of graphene.

Figure S1(c) represents the FTIR spectra of graphite, graphene oxide and GQD as recorded within wavenumber from 4000 to 600 cm^{-1}. Generally, the spectra reveal the presence of oxygen containing functional groups attached to the all carbon honeycomb core. In the presented spectra, there are no peaks for graphite, which is obvious as graphite is devoid of any functionality. Graphite being the starting material presents a good reference point as how step by step the functionality is introduced with the successive step in order to synthesize GQD. Graphene oxide, which was synthesized from graphite by oxidative exfoliation. we observe characteristic peaks corresponding to the –OH at 3200–3600 cm^{-1}, C=O (1670–1820 cm^{-1}), -COC- at 1000–1300 cm^{-1}. These are the usual defects which are introduced by oxidative exfoliation in the graphitic and graphene plane [34]. GQD are synthesized by hydrothermal cutting of GO sheets along the ethoxy functionality as discussed by Pan et al. [2] This leads to the formation of smaller size quantum dots with excitonic entrapment in all the three spatial dimension. What it also does is introduce an edge with certain functional groups which may be seen in the FTIR spectrum of GQD. As the GOQ is formed due to the breaking of -COC- linkage, we only observe peaks corresponding to the –OH at 3200–3600 cm^{-1}, C=O (1670–1820 cm^{-1}). These peaks indicate the presence of -COOH, -CO and -OH terminating edges of GQD. Further, these groups play an important role in binding with nitrogen during the amination step which leads to the formation of NH_2-GQD. Figure S1(d) compares the FTIR spectra of GQD and NH_2-GQD-GO. Broad -OH peak at 3450 cm^{-1} in the spectra of GQD widens further and shift towards 3500 cm^{-1} in NH_2-GQD-GO due to merging with -NH stretching peak which is indicative of amino functionalization of GQD by forming -$CONH_2$ bonds over the surface of GQD [35]. This is further strengthened by the presence of -NH bending peak at 1382 cm^{-1}. These results hence help us understand a clear pathway which is being followed to obtain NH_2-GQD from graphite. Additionally, the role of edge become even more important in both GQD and NH_2-GQD because they dominate the properties of their graphene core. This dominance of the edges over the core is much more evident when the Raman spectra of GQD was observed in correlation to the information obtained by the TEM. Raman analysis (Figure S2) of GQD presented the characteristic D band and G band associated with graphene at 1350 cm^{-1} and 1580 cm^{-1} respectively. The D band arise due to the disordered C atoms at the edges of the GQD, whereas the G band is observed due to the in-plane vibration of sp^2-bonded C atoms, respectively [36]. The equal intensity of both bands indicates the appreciable loss of graphitic layered structure. It can be interpreted as the GOQ synthesized is either single or few layers (mostly bi- or tri-) in nature. However, it was revealed in TEM that the core of the GQD are much darker in color suggesting it to have more than three layers. This anomaly is because the GQD are more defective than the graphene sheets owing to their dominating edge effect. Therefore, the intensity ratio is not the ideal parameter to estimate the number of layers of the quantum dots [37].

The NH_2-GQD synthesized via hydrothermal cutting of GO can be visualized in the TEM micrograph (Fig. 1(a)). The average size of the dots from TEM was found to be 22 nm (Inset Fig. 1(a)). This was analyzed by the means of image analysis by ImageJ software developed by Wayne Rasband (https://imagej.nih.gov/ij/). The result reflects data collected from 52 quantum dots in the image with the minimum size of 12 nm, maximum of 37 nm and standard

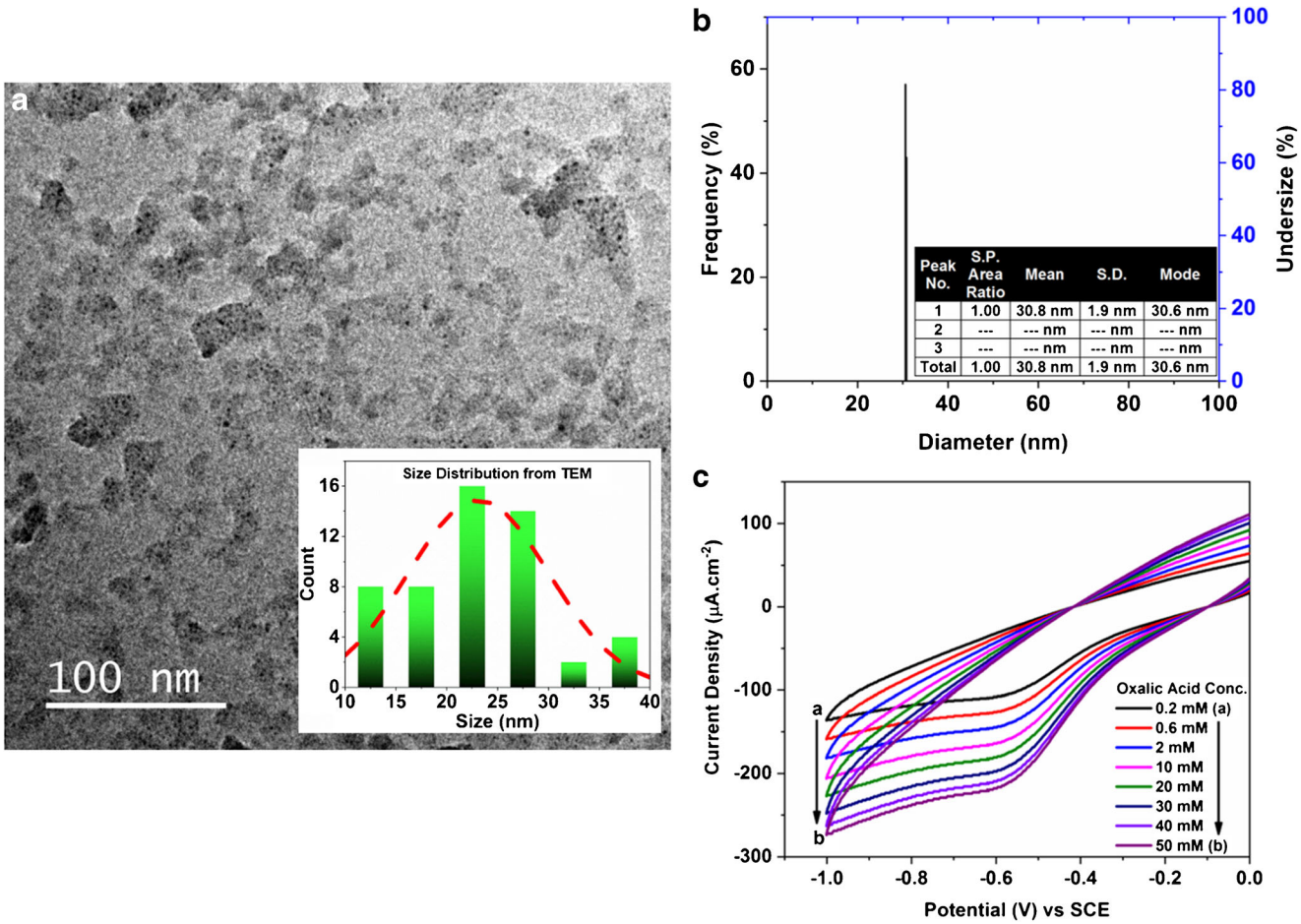

Fig. 1 **a** Transmission electron micrograph of NH_2-GQD (Inset Particle Size of Distribution of NH_2-GQD from TEM); **b** Particle size analysis of NH_2-GQD. **c** Cyclic voltagram of NH_2-GQD-GO with addition of variable concentration of oxalic acid recorded within −1.0 V to 0 V at 50 mV.s^{-1}

deviation of 7.2 nm. Many of the NH_2-GQD also presents very dark core. This is due to the multiple graphitic layers which constitute the quantum dot. The average particle size of the NH_2-GQD was also determined by the particle size analyzer with the quantum dots dispersed in ethanol (Fig. 1(b)). The size of the GQD was found to be 30 nm which is in near approximation to the size obtained by TEM image analysis. Moreover, observation of larger size is also due to the solvent barrier formed around the dots due to H-bonding between the solvent molecule and the quantum dots. The reason for this interaction is the presence of oxygen containing functional groups on the edge of the GQD. This is also evident from the FTIR spectra of the quantum dot (Figure S1(d)). Moreover, this edge effect is later shown to play an important role in the electrochemistry of NH_2-GQD.

Therefore, on close characterization of GQD and NH_2-GQD, it was observed that the quantum dots are well covered with functional groups bearing electronegative centers (i.e. either O or N) on the edges. This in turn lead to the hypothesis that they should exhibit their electrochemical property in the reductive cycle or the cathodic sweep of the cyclic voltammetry. In subsequent section, a discussion is made on how these quantum dots express themselves in the cathodic cycle, and how this property may be used to detect oxalic acid in the aqueous media.

Electrochemical sensing of oxalic acid

Electrochemical properties of NH_2-GQD, and NH_2-GQD-GO composite are evaluated using cyclic voltammetry, with the potential range of −1.2 V to 0.5 V. The oxidation and reduction potentials were determined by plotting a graph of current density against the applied voltage. GQD, NH_2-GQD, and NH_2-GQD-GO shows distinct cathodic peak at −0.6 V (Figure S3(a)). This is due to the reduction of carboxyl and carbonyl groups present over the edge of the quantum dots. The reduction in the cathodic current density observed in the CV curve as we go from GQD to NH_2-GQD is due to the availability of lesser number of carboxylic groups per gram of the overall nanostructure, which is in the following order:

$$NH_2\text{−GQD−GO} < NH_2\text{−GQD} < \text{GQD}$$

The dependence of the cathodic current density on the availability of carboxylic group is further strengthen by the fact that GO, although have large number of carbonyl and ethoxy group fails to improve the cathodic current density when composited with NH_2-GQD. There was no cathodic peak observed at −0.6 V in the CV of GO (Figure S3(d)). Therefore, it may be understood that the increase in the number of carboxylic groups in the GQD system is directly related to the increase the cathodic current density observed at the said potential. This information prompted the attempt to use the NH_2-GQD-GO composite for the determination of oxalic acid.

Figure S3(b to e), shows the variation in the cathodic current density observed for the GC electrode deposited with GQD, NH_2-GQD, GO, and NH_2-GQD-GO, respectively, with and without the addition of 2 mM oxalic acid. As evident from the cyclic voltagram, there is no significant change in the observed currents at the applied potential range for GQD and NH_2-GQD. In case of GO, there is no cathodic peak observed when oxalic acid was added to the electrolyte. The cathodic peak observed in GO without oxalic acid is due to the reduction of GO to graphene [38]. However, in case of NH_2-GQD-GO, the addition of oxalic acid showed a significant increase in the cathodic current density. This highlights the need of amination of GQD. The potential sweep window was shortened for the composite after it was established that the cathodic peak occurs at −0.6 V to have better resolution of the two voltagram. The edges of GQD are saturated with oxygen rich groups which results in no significant raise in the cathodic current density when oxalic acid is added as it does not get binding sites on the edge and additionally the low amount of binding which occur is not enough to induce a variation in the current density. The amination of the GQD edges reduce the oxygen rich groups on the edge and therefore NH_2-GQD-GO composite showed lower cathodic current density of all (Figure S4(a)). Additionally, the presence of NH_2 groups on the edges of the quantum dots help in binding with oxalic acid thereby increasing the number of acid groups on the edges available for reduction which increase the reduction current density. The mechanism for the change in cathodic current may be visualized from Scheme 1. As oxalic acid is a dicarboxylic acid, it forms an amide linkage with the amino groups present in NH_2-GQD-GO leading to free carboxylic group on the surface available for reduction at −0.6 V. Therefore, it can be seen as a case where, the oxalic acid increases the number of carboxylic groups on the surface of the NH_2-GQD-GO. However, this is not observed to happen in NH_2-GQD deposited GC electrode as there is no substrate available to facilitate the formation of amide linkage. This is where the need of forming NH_2-GQD-GO composite is highlighted. GO owing to its large surface area provides the platform for the formation of amide linkage between amino groups of NH_2-GQD and carboxylic group of oxalic acid. Hence, in a nutshell, the presence of oxalic acid provides extra carboxylic groups when bonded to NH_2-GQD-GO which further undergo deprotonation at the said potential leading to an increase in the cathodic current density. This dependence of cathodic current density observed in the NH_2-GQD-GO/GC electrode system on the concentration of oxalic acid led to the exploration of the system for the electrochemical determination of oxalic acid. This may be taken up as the foundation for the development of NH_2-GQD-GO based electrochemical sensor for oxalic acid.

The suitability of an electrochemical sensor relies in its ability to quantitatively analyze the presence of the analyte. It was found that this increase in cathodic current density is concentration dependent (Fig. 1(c)). The consecutive cyclic voltagram of NH_2-GQD-GO/GC electrode with the addition of incremental concentration of oxalic acid shows that there is an increase in cathodic current density.

The nature of this variation is found to be linear with two different slopes which can be seen from Fig. 2. Figure 2(a) represents the variation in cathodic current density with the concentration of oxalic acid from 0.05 mM to 2 mM. The Fig. 2(b) shows that within this range of concentration of oxalic acid, the cathodic current density was found to be linearly increasing within 0.5 mM to 2 mM of oxalic acid with the goodness of fit (R^2) of 0.96 and standard deviation (SD) of 12.9. The sensitivity of the electrode for this range was calculated to be 129.502 $\mu A.mM^{-1}.cm^{-2}$. Similarly, Fig. 2(c) represents the variation in cathodic current density with the concentration of oxalic acid from 0.2 mM to 55 mM, with the linear variation of the cathodic current density within 2.0 mM to 55 mM concentration of oxalic acid (Fig. 2(d)) having R^2 as 0.98 and SD of 38.05. The sensitivity of the electrode for this range was found to be 142.253 $\mu A.mM^{-1}.cm^{-2}$. The limit of detection of oxalic acid for the electrode was found to be 0.05 mM, which is based on the lower limit of the oxalic acid which resulted in a variation of current density at −0.6 V by 12.9 μA (SD of the analysis for oxalic acid concentration between 0.05–2.0 mM) after 3 trials. The shaded region of the plot resembles the SD expanse for the data point with the darker region (confidence range) being the limit of ± SD and the lighter region (prediction range) corresponds to the limit of ±3SD. The determination of the current densities w.r.t the concentration of the oxalic acid considered to be statistically accepted as all the data points lie within the prediction range (i.e. follow the 3SD rule, whereby 95% of all the data should lie between the ±3SD from the mean).

Table 1 gives a comparison of presented electrode with other electrodes reported in the literature. Bare platinum and platinum nanoparticles deposited on GC electrode still provides lowest LOD among the reported electrodes developed for the electrochemical determination of oxalic acid. NH_2-GQD-GO/GC electrode have widest linear range among all the electrodes. Moreover, the all carbon architecture makes

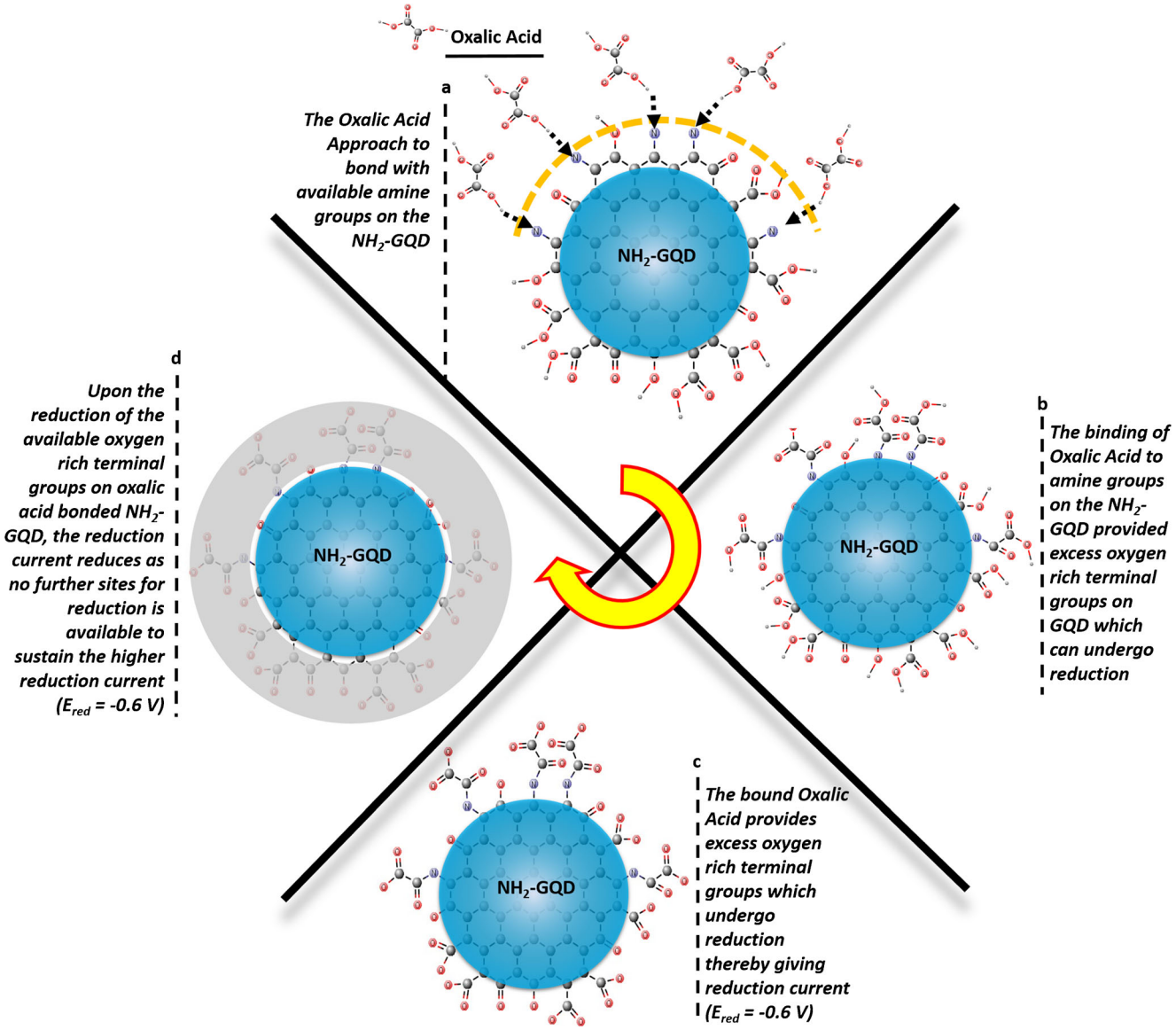

Scheme 1 Plausible mechanism of binding between NH_2-GQD and oxalic acid and subsequent electro-reduction at $E_{red} = -0.6$ V.

its most economical among all the other reported electrodes for the electrochemical determination of oxalic acid. Another first for this electrode is the use of cathodic current density (reductive cycle) for the determination oxalic acid. To the best of our knowledge, all the other electrochemical methods of determination of oxalic acid is cathodic current density (Oxidative cycle) based. This opens up the possibility to determine the analytes with materials which have predominately electron rich centers. In the presented study, oxalic acid (analyte) and active sensing material (NH_2-GQD) are have O and N centers. Oxalic acid being dicarboxylic acid have two protons available to be released. The NH_2-GQD have edges laden with -NH_2, -CO and -COOH group. Among this the -NH_2 moiety binds with available oxalic acid to form amide linkage. The second carboxylic acid group here is then free to undergo deprotonation. Therefore, in presence of oxalic acid there is an increase in -COOH on NH_2-GQD which undergo deprotonation at the said potential, thereby giving a rise in cathodic current density.

The quickness of the electrode to determine the presence of the analyte also contribute towards the sensitivity of the sensor to ascertain its efficiency. Apart from sensitivity, the selectivity of the electrode is also essential. To study these, the chronoamperometric behavior of NH_2-GQD-GO was studied with the addition of oxalic acid during the scan to calculate the response time (Fig. 3(a)), and with the addition of oxalic acid, glucose and uric acid during the scan (Fig. 3(b)) for the interference study. Glucose (0.5 M) and uric acid (0.5 M) were selected as interfering agents as they are the other components which are usually present in urine sample which are analyzed for the determination of oxalic acid (or oxalate) in humans. This study reveals that the electrode is very

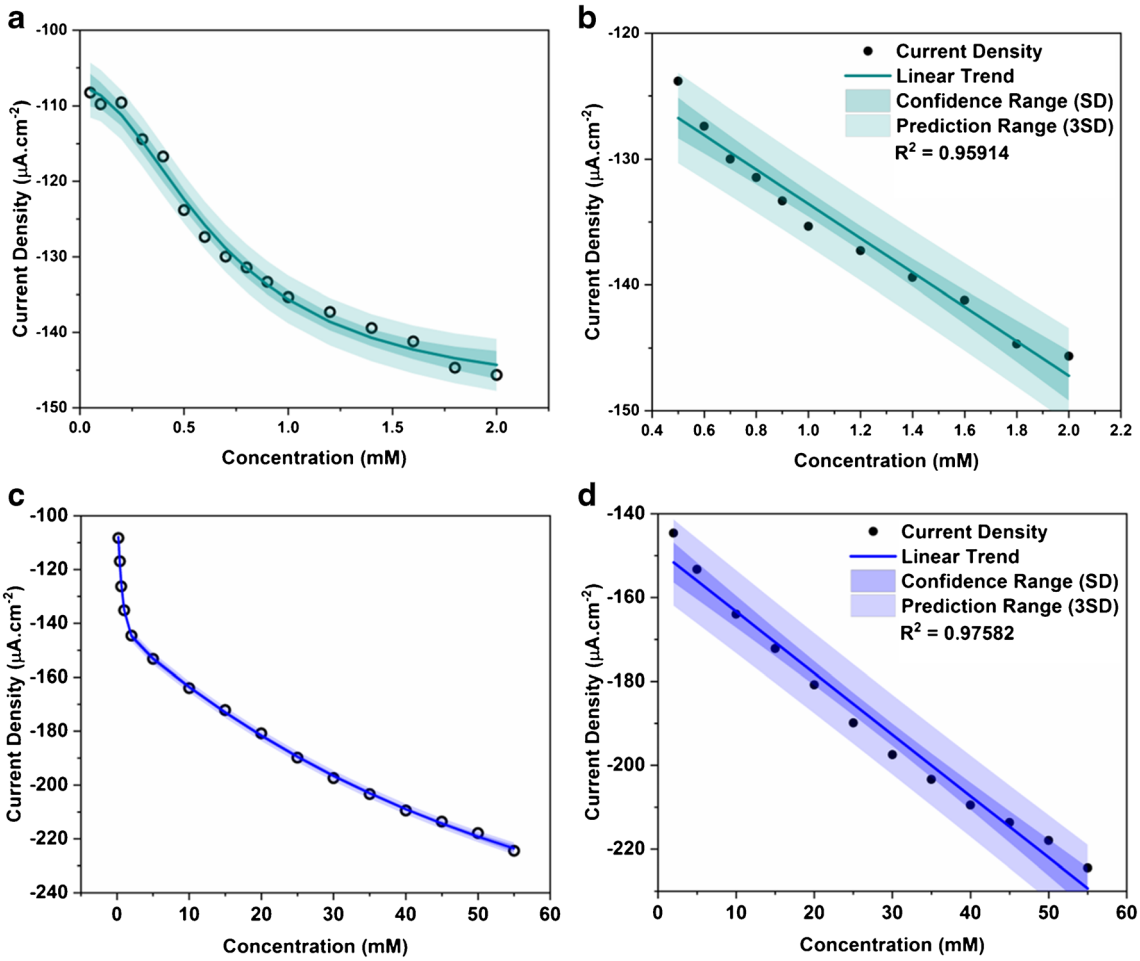

Fig. 2 Variation of cathodic current density within (**a**) 0.01–2 mM concentration of Oxalic acid, and (**b**) the linear variation of the current density between 0.5–2.0 mM concentration of Oxalic acid; Variation of cathodic current density within (**c**) 0.01–55 mM concentration of Oxalic acid, and (**d**) the linear variation of the current density between 2.0–55 mM concentration of Oxalic acid

responsive towards the presence of oxalic acid with a response time of mere 2 s. The interference study shows that the observed change in cathodic peak on addition of oxalic acid is significantly very large compared to the addition of glucose or uric acid.

Determination of oxalic acid in real sample

The urine samples were studied to determine the oxalic acid content by the collecting from an average male [31]. Additionally, spinach extract was also studied for its oxalic

Table 1 The parameter of NH_2-GQD-GO/GC electrode for electrochemical determination of oxalic acid in comparison to other electrodes reported in literature

Electrode	Sensitivity ($\mu A.mM^{-1}.cm^{-2}$)	Linear Range (up to, mM)	LOD (μM)	Potential (V)	Ref.
Bare Pt electrode	NA	0.57×10^{-3} to 104.01×10^{-3} 104.01×10^{-3} to 228.75×10^{-3}	0.38	0.9	[27]
Pt-nanoparticles/GC	NA	1.14×10^{-3} to 342.80×10^{-3} 342.80×10^{-3} to 548.92×10^{-3}	0.28	0.95	
Graphene modified carbon ionic liquid electrode	NA	8 × 10 to 3–6.0	48	1.34	[28]
Pd-CNF/CPE	NA	0.2 to 13 13 to 45	20	1.10	[29]
NH_2-GQD-GO/GC	129.502 142.253	0.5 to 2.0 2.0 to 55.0	50	−0.65	This work

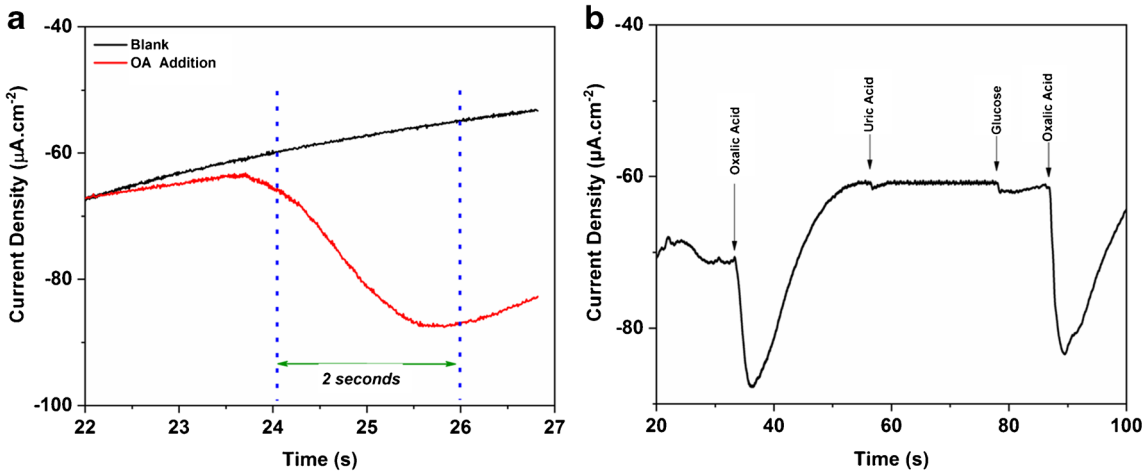

Fig. 3 **a** Chronoamperometric response of NH_2-GQD-GO on addition of 2 mM Oxalic acid and **b** Variation in cathodic current density on addition of Oxalic acid, uric acid, and glucose

acid content. This was done to study the practical applicability of the sensor. To confirm the practical applicability of the sensor, urine was used as a real sample and the experiment was conducted. The 2 mL urine sample was added to the 20 mL buffered electrolyte at pH 7.4, to which the NH_2-GQD-GO/GC electrode was dipped as working electrode with Pt wire as counter electrode and saturated calomel electrode as reference electrode. The estimation of the sample was done substituting the current density obtained at −0.6 V in the calibration plot depicted in figure 2(b). The concentration was found to be 0.55 mM which is equivalent to 49 $mg.L^{-1}$ of the urine sample which is around the average limit of oxalic acid in urine. These levels of oxalic acid in urine were in agreement with the clinical determination of urine sample (47 $mg.L^{-1}$). In a separate experiment, the spinach extract was prepared by crushing 100 g spinach leaves in mortar pestle and then dissolving them in water followed by filtration. The aliquot was used for further analysis. 2 mL aliquot was added to 20 mL buffered electrolyte and studied as per the earlier described procedure. The content of oxalic acid was found to be 1.5 mM which is equivalent to 135 $mg.L^{-1}$ of aliquot.

Therefore, the electrochemical results of the NH_2-GQD-GO/GC electrode make it evident that it is very accurate in determining the concentration of oxalic acid in wide concentration range of 0.5 mM to 55 mM with very quick response. It is also relatively non-responsive towards other interfering molecules that might be present in certain chemical and biological samples. This phenomenon can be utilized in generating a non-enzymatic sensor for oxalic acid. However, the control over the size of the NH_2-GQD synthesized by the hydrothermal method effects the activity of the sensor. All the results reported here were performed using the NH_2-GQD-GO composite made of single batch of NH_2-GQD. As the reported method make use of the di-basic nature of oxalic acid for its determination, there is high possibility of the interference from other bi-basic acids if present in the sample. Lastly, the amide bonding between the oxalic acid and -NH2 group present on the surface of NH_2-GQD-GO is irreversible. Therefore, these electrodes can only be utilized as single use probe.

Conclusions

A nanocomposite of type NH_2-GQD-GO is described that exhibits good electrochemical response to oxalate in cathodic sweep cyclic voltammetry, with a peak cathodic current at −0.6 V. The NH_2-GQD-GO readily binds with di-basic acids like oxalic acid due to the active surface provided by the host GO to -NH2 groups of the functionalized GQD to bind with one carboxylic group of the di-basic carboxylic acid. Therefore, the cathodic current density at −0.6 V is dependent on the concentration of oxalic acid bound to the surface of NH_2-GQD-GO due to the electro reduction of carboxylic group. Additionally, the composite is electroactive in mild basic pH which correlates to the pH of urine sample. Therefore, the composite is suitable for the determination of oxalic acid in dual linear range of 0.5 mM to 2.0 mM and 2.0 mM to 55 mM oxalic acid with the LOD of 0.05 mM. Moreover, the presented work illustrates the use the cathodic current density for quantitatively determining the analyte in chemical and biological samples. This can be extended to further develop a non-enzymatic biosensor for the determination of oxalic acid in food, vegetables and other biological samples. However, the strict control on the size of synthesized functionalized GQD which limits the activity of the composite, and one-time use of electrode are the limitations which requires further attention.

Acknowledgements Mr. Praveen Mishra is thankful for the financial and infrastructural support extended by the National Institute of Technology Karnataka, Surathkal, Mangalore.

Compliance with ethical standards All procedures performed in studies involving human participants were in accordance with the ethical standards of the institutional research committee and with the 1964 Helsinki declaration and its later amendments or comparable ethical standards.

References

1. Shen J, Zhu Y, Yang X, Li C (2012) Graphene quantum dots: emergent nanolights for bioimaging, sensors, catalysis and photovoltaic devices. Chem Commun 48(31):3686–3699. https://doi.org/10.1039/C2CC00110A
2. Pan D, Zhang J, Li Z, Wu M (2010) Hydrothermal route for cutting graphene sheets into blue-luminescent graphene quantum dots. Adv Mater 22(6):734–738. https://doi.org/10.1002/adma.200902825
3. Yan X, Cui X, Li B, Li L-s (2010) Large, solution-Processable graphene quantum dots as light absorbers for photovoltaics. Nano Lett 10(5):1869–1873. https://doi.org/10.1021/nl101060h
4. Benítez-Martínez S, Valcárcel M (2015) Graphene quantum dots in analytical science. TrAC Trends Anal Chem 72 (Supplement C:93–113. https://doi.org/10.1016/j.trac.2015.03.020
5. Dong Y, Li G, Zhou N, Wang R, Chi Y, Chen G (2012) Graphene quantum dot as a green and facile sensor for free chlorine in drinking water. Anal Chem 84(19):8378–8382. https://doi.org/10.1021/ac301945z
6. Zhao J, Chen G, Zhu L, Li G (2011) Graphene quantum dots-based platform for the fabrication of electrochemical biosensors. Electrochem Commun 13(1):31–33. https://doi.org/10.1016/j.elecom.2010.11.005
7. Xu H, Zhou S, Xiao L, Wang H, Li S, Yuan Q (2015) Fabrication of a nitrogen-doped graphene quantum dot from MOF-derived porous carbon and its application for highly selective fluorescence detection of Fe3+. J Mater Chem C 3(2):291–297. https://doi.org/10.1039/C4TC01991A
8. Liu X, Gao W, Zhou X, Ma Y (2014) Pristine graphene quantum dots for detection of copper ions. J Mater Res 29(13):1401–1407. https://doi.org/10.1557/jmr.2014.145
9. Fan Z, Li Y, Li X, Fan L, Zhou S, Fang D, Yang S (2014) Surrounding media sensitive photoluminescence of boron-doped graphene quantum dots for highly fluorescent dyed crystals, chemical sensing and bioimaging. Carbon 70 (Supplement C:149–156. https://doi.org/10.1016/j.carbon.2013.12.085
10. Cai F, Liu X, Liu S, Liu H, Huang Y (2014) A simple one-pot synthesis of highly fluorescent nitrogen-doped graphene quantum dots for the detection of Cr(vi) in aqueous media. RSC Adv 4(94):52016–52022. https://doi.org/10.1039/C4RA09320H
11. Huang H, Liao L, Xu X, Zou M, Liu F, Li N (2013) The electron-transfer based interaction between transition metal ions and photoluminescent graphene quantum dots (GQDs): a platform for metal ion sensing. Talanta 117(Supplement C):152–157. https://doi.org/10.1016/j.talanta.2013.08.055
12. Hallaj T, Amjadi M, Manzoori JL, Shokri R (2015) Chemiluminescence reaction of glucose-derived graphene quantum dots with hypochlorite, and its application to the determination of free chlorine. Microchim Acta 182(3):789–796. https://doi.org/10.1007/s00604-014-1389-0
13. Bai J-M, Zhang L, Liang R-P, Qiu J-D (2013) Graphene quantum dots combined with europium ions as Photoluminescent probes for phosphate sensing. Chem Eur J 19(12):3822–3826. https://doi.org/10.1002/chem.201204295
14. Roushani M, Abdi Z (2014) Novel electrochemical sensor based on graphene quantum dots/riboflavin nanocomposite for the detection of persulfate. Sensors Actuators B Chem 201 (Supplement C:503–510. https://doi.org/10.1016/j.snb.2014.05.054
15. Sun R, Wang Y, Ni Y, Kokot S (2014) Graphene quantum dots and the resonance light scattering technique for trace analysis of phenol in different water samples. Talanta 125(Supplement C):341–346. https://doi.org/10.1016/j.talanta.2014.03.007
16. Zhang L, Zhang Z-Y, Liang R-P, Li Y-H, Qiu J-D (2014) Boron-doped graphene quantum dots for selective glucose sensing based on the "abnormal" aggregation-induced photoluminescence enhancement. Anal Chem 86(9):4423–4430. https://doi.org/10.1021/ac500289c
17. Liu J-J, Zhang X-L, Cong Z-X, Chen Z-T, Yang H-H, Chen G-N (2013) Glutathione-functionalized graphene quantum dots as selective fluorescent probes for phosphate-containing metabolites. Nanoscale 5(5):1810–1815. https://doi.org/10.1039/C3NR33794D
18. Koch GH, Strong FM (1969) Determination of oxalate in urine. Anal Biochem 27(1):162–171. https://doi.org/10.1016/0003-2697(69)90227-9
19. Tadi KK, Motghare RV (2013) Potentiometric selective recognition of oxalic acid based on molecularly imprinted polymer. Int J Electrochem Sci 8:3197–3211
20. Bergerman J, Elliot JS (1955) Method for direct colorimetric determination of oxalic acid. Anal Chem 27(6):1014–1015. https://doi.org/10.1021/ac60102a045
21. Zarembski PM, Hodgkinson A (1965) The fluorimetric determination of oxalic acid in blood and other biological materials. Biochem J 96(3):717–721
22. He Z, Gao H (1997) Simultaneous determination of oxalic and tartaric acid with Chemiluminescence detection. Analyst 122(11):1343–1346. https://doi.org/10.1039/A702953E
23. Costello J, Hatch M, Bourke E (1976) An enzymic method for the spectrophotometric determination of oxalic acid. J Lab Clin Med 87(5):903–908. https://doi.org/10.5555/uri:pii:0022214376904662
24. Fry IDR, Starkey BJ (1991) The determination of oxalate in urine and plasma by high performance liquid chromatography. Ann Clin Biochem 28(6):581–587. https://doi.org/10.1177/000456329102800607
25. Pfeiffer K, Berg W, Bongartz D, Hesse A (1997) The direct determination of urinary oxalate by non-suppressed ion chromatography. https://doi.org/10.1515/cclm.1997.35.4.305
26. Trevaskis M, Trenerry VC (1996) An investigation into the determination of oxalic acid in vegetables by capillary electrophoresis. Food Chem 57(2):323–330. https://doi.org/10.1016/0308-8146(95)00228-6
27. Ma L, Zeng Q, Zhang M, Wang L, Cheng F (2016) Direct determination of oxalic acid by a bare platinum electrode contrasting a platinum nanoparticles-modified glassy carbon electrode. J Exp Nanosci 11(16):1242–1252. https://doi.org/10.1080/17458080.2016.1209586
28. Wang X, Cheng Y, You Z, Sha H, Gong S, Liu J, Sun W (2015) Sensitive electrochemical determination of oxalic acid in spinach samples by a graphene-modified carbon ionic liquid electrode. Ionics 21(3):877–884. https://doi.org/10.1007/s11581-014-1233-x
29. Liu Y, Huang J, Wang D, Hou H, You T (2010) Electrochemical determination of oxalic acid using palladium nanoparticle-loaded carbon nanofiber modified electrode. Anal Methods 2(7):855–859. https://doi.org/10.1039/C0AY00098A
30. Kim W, Lee JS, Shin DH, Jang J (2018) Platinum nanoparticles immobilized on polypyrrole nanofibers for non-enzyme oxalic acid sensor. J Mater Chem B 6(8):1272–1278. https://doi.org/10.1039/C7TB00629B
31. Pan F, Chen D, Zhuang X, Wu X, Luan F, Zhang S, Wei J, Xia S, Li X (2018) Fabrication of gold nanoparticles/l-cysteine functionalized graphene oxide nanocomposites and application for nitrite detection. J Alloys Compd 744:51–56. https://doi.org/10.1016/j.jallcom.2018.02.053

32. Marcano DC, Kosynkin DV, Berlin JM, Sinitskii A, Sun Z, Slesarev A, Alemany LB, Lu W, Tour JM (2010) Improved synthesis of graphene oxide. ACS Nano 4(8):4806–4814. https://doi.org/10.1021/nn1006368
33. Li B, Nan Y, Zhang P, Song X (2016) Structural characterization of individual graphene sheets formed by arc discharge and their growth mechanisms. RSC Adv 6(24):19797–19806. https://doi.org/10.1039/C5RA23990G
34. Hummers WS, Offeman RE (1958) Preparation of graphitic oxide. J Am Chem Soc 80(6):1339–1339. https://doi.org/10.1021/ja01539a017
35. Zhu X, Zuo X, Hu R, Xiao X, Liang Y, Nan J (2014) Hydrothermal synthesis of two photoluminescent nitrogen-doped graphene quantum dots emitted green and khaki luminescence. Mater Chem Phys 147(3):963–967. https://doi.org/10.1016/j.matchemphys.2014.06.043
36. Hu C, Liu Y, Yang Y, Cui J, Huang Z, Wang Y, Yang L, Wang H, Xiao Y, Rong J (2013) One-step preparation of nitrogen-doped graphene quantum dots from oxidized debris of graphene oxide. J Mater Chem B 1(1):39–42. https://doi.org/10.1039/C2TB00189F
37. Kim S, Shin DH, Kim CO, Kang SS, Joo SS, Choi S-H, Hwang SW, Sone C (2013) Size-dependence of Raman scattering from graphene quantum dots: interplay between shape and thickness. Appl Phys Lett 102(5):053108. https://doi.org/10.1063/1.4790641
38. Yang J, Deng S, Lei J, Ju H, Gunasekaran S (2011) Electrochemical synthesis of reduced graphene sheet–AuPd alloy nanoparticle composites for enzymatic biosensing. Biosens Bioelectron 29(1):159–166. https://doi.org/10.1016/j.bios.2011.08.011